Supporting Information

Wu et al. 10.1073/pnas.1320753111

SI Materials and Methods

Isolation of Mononuclear Cells from Peripheral Blood and Tissues. Peripheral leukocytes were isolated by Ficoll density gradient centrifugation. Fresh tumor and peritumor and normal mucosa infiltrating leukocytes were obtained as described in our previous studies (1–4). In short, colon tissue biopsy specimens ($n = 8$) were cut into small pieces and digested in RPMI 1640 supplemented with 0.05% collagenase Type IV (Sigma-Aldrich), 0.002% DNase I (Roche), and 20% (vol/vol) FCS (HyClone). The dissociated cells were then filtered through a 150-μm mesh, and the mononuclear cells were obtained by Ficoll density gradient centrifugation. The mononuclear cells were washed and resuspended in media supplemented with 1% heat-inactivated FCS for FACS analysis.

Flow Cytometry Analysis. For surface marker staining, the cells were prepared and suspended in PBS solution supplemented with 1% heat-inactivated FCS. For intracellular staining, the cells were fixed and permeabilized with IntraPre Reagent (Beckman Coulter). An APC anti-Foxp3 Staining Set (eBioscience) was used for Foxp3 analysis according to the manufacturer's instructions. Data were acquired on a Gallios flow cytometer (Beckman Coulter) and analyzed with FlowJo software. The fluorochrome-conjugated Abs used are summarized in Table S2.

ELISA. The concentrations of serum G-CSF and GM-CSF in the patient samples were detected with high-sensitivity ELISA kits (R&D Systems), and the concentrations of IFN-γ in the culture supernatants were detected by ELISA kits (eBioscience).

Immunofluorescence. Paraffin-embedded and frozen colon cancer samples were cut into 5-μm sections and processed for immunofluorescence as previously described (1, 2). The tissues were stained with mouse anti-human CD34, rabbit anti-human CD133 (Abcam), rabbit anti-human CXCR4 (Epitomics), or mouse anti-human CD15 (Thermo Scientific), followed by Alexa Fluor 488-conjugated goat anti-mouse IgG and Alexa Fluor 568- or 555-conjugated goat anti-rabbit IgG (Life Technologies). The nuclei were stained with DAPI. The images were viewed by using a scanning confocal microscope (Leica) at wavelengths of 488 and 546 nm and analyzed with LAS AF Lite software.

In Vitro Methylcellulose Colony-Forming Cell Assay. $Lin^{-}CD34^{+}$ cells were purified from equal amounts (5 mL) of peripheral blood by using a Diamond CD34 Isolation Kit (Miltenyi Biotec). The isolated cells were plated and cultured in Methocult H4034 (StemCell Technologies). Colonies were assigned scores after 14–16 d of culture according to criteria in the technical manual provided with the assay media (StemCell Technologies). The types and frequency of colonies were compared between healthy donors and patients with cancer.

Expansion of Human Cord Blood $CD34^{+}$ Cells and Generation of Cord Blood-Derived Myeloid-Derived Suppressor Cells. $CD34^{+}$ cells were purified from fresh human cord blood (CB) by using a direct CD34 progenitor cell isolation kit, according to the manufacturer's instructions (Miltenyi Biotec). These $CD34^{+}$ cells were plated at 5×10^4 cells per milliliter per well in U-bottom 96-well plates (Corning) with 200 μL of hematopoietic stem cell (HSC) expansion media (StemSpan SFEM; Stem Cell Technologies) supplemented with 100 ng/mL stem cell factor, 100 ng/mL Fms-like tyrosine kinase 3, 100 ng/mL thrombopoietin, and 20 ng/mL IL-3 (R&D Systems) (5). The cells were cultured at 37 °C in 5% CO_2. On day 3, the cells were pooled and transferred to six-well plates, and fresh media was added on days 3, 5, and 7 to keep the cell density at 1×10^5 cells per milliliter (day 3), 5×10^5 cells per milliliter (day 5), and 7.5×10^5 cells per milliliter (day 7). To obtain CB-derived myeloid-derived suppressor cells (MDSCs), the expanded $CD34^{+}$ cells were plated at 5×10^5 per well in 24-well plates in complete RPMI medium supplemented with GM-CSF (40 ng/mL), G-CSF (40 ng/mL), or IL-6 (40 ng/mL), and cultured at 37 °C in 5% CO_2-humidified atmosphere for 3–4 d (6).

Coculture of CB-Derived MDSCs with Pan T Cells. Pan-T cells were purified from peripheral blood of healthy donors using a Pan-T Cell Isolation Kit (Miltenyi Biotec). These cells were left untreated or were cocultured with CB-derived MDSCs (CB-MDSCs; 1:1 ratio) in the presence of 1 μg/mL coated anti-CD3 and 5 μg/mL soluble anti-CD28 for 6 d at 37 °C in a 5% CO_2-humidified atmosphere (6, 7). In some experiments, the T cells were stained with 2.5 μM carboxyfluorescein diacetate succinimidyl ester before stimulation, according to the manufacturer's instructions (Invitrogen Molecular Probe). Subsequently, the cells were analyzed by flow cytometry, and the concentration of IFN-γ in the supernatant was determined by ELISA.

Statistical Analysis. The results are expressed as means ± SEM. The statistical significance of the differences between groups was determined by Student t test, nonparametric Mann–Whitney U test, or one-way ANOVA as appropriate. The cumulative survival time was calculated by the Kaplan–Meier method, using the median value as a cutoff to separate patients into high and low groups (2). Survival was measured in months from treatment to progression or the last review (8). The log-rank test was applied to compare the groups. All data were analyzed by using two-tailed tests unless otherwise specified, and $P < 0.05$ was considered statistically significant.

1. Kuang DM, et al. (2007) Tumor-derived hyaluronan induces formation of immunosuppressive macrophages through transient early activation of monocytes. *Blood* 110(2):587–595.
2. Kuang DM, et al. (2009) Activated monocytes in peritumoral stroma of hepatocellular carcinoma foster immune privilege and disease progression through PD-L1. *J Exp Med* 206(6):1327–1337.
3. Wu Y, et al. (2013) Monocyte/macrophage-elicited natural killer cell dysfunction in hepatocellular carcinoma is mediated by CD48/2B4 interactions. *Hepatology* 57(3):1107–1116.
4. Kuang DM, et al. (2008) Tumor-educated tolerogenic dendritic cells induce CD3epsilon down-regulation and apoptosis of T cells through oxygen-dependent pathways. *J Immunol* 181(5):3089–3098.
5. Boitano AE, et al. (2010) Aryl hydrocarbon receptor antagonists promote the expansion of human hematopoietic stem cells. *Science* 329(5997):1345–1348.
6. Marigo I, et al. (2010) Tumor-induced tolerance and immune suppression depend on the C/EBPbeta transcription factor. *Immunity* 32(6):790–802.
7. Corzo CA, et al. (2010) HIF-1α regulates function and differentiation of myeloid-derived suppressor cells in the tumor microenvironment. *J Exp Med* 207(11):2439–2453.
8. Liao Y, et al. (2013) Increased circulating Th17 cells after transarterial chemoembolization correlate with improved survival in stage III hepatocellular carcinoma: A prospective study. *PLoS ONE* 8(4):e60444.

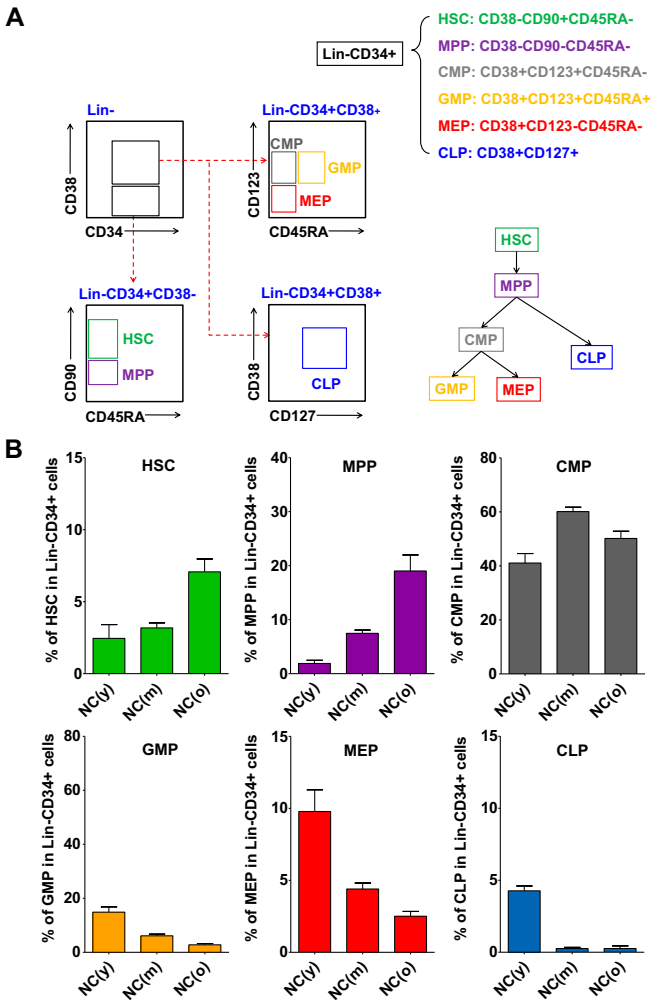

Fig. S1. Gating strategy and the frequency of hematopoietic stem and progenitor cells (HSPCs) in the peripheral blood from different ages of healthy donors. (*A*) Gating strategy for FACS analysis of the frequency of HSPC subsets in the $Lin^{-}CD34^{+}$ population from healthy adults and patients with cancer. (*B*) Summary of HSCs, multipotent progenitors (MPP), common myeloid progenitors (CMP), granulocyte–monocyte progenitors (GMPs), megakaryocyte–erythroid progenitors (MEP), and common lymphoid progenitors (CLP) in the total $Lin^{-}CD34^{+}$ population from the peripheral blood samples of healthy young (age 20–35 y; $n = 7$), middle age (age 36–65 y; $n = 42$), or elderly (age ≥65 y; $n = 14$) adults.

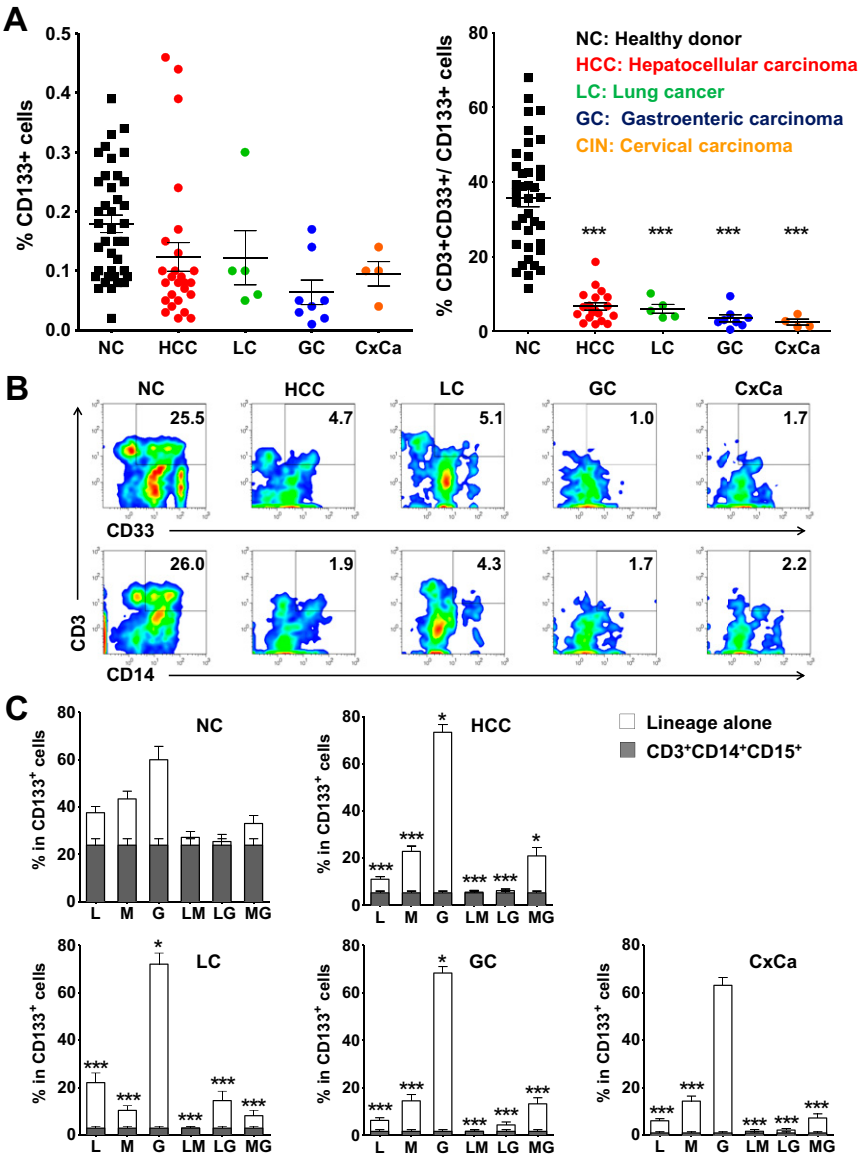

Fig. S2. The frequency of circulating precursors with potential to differentiate into lymphocytes is reduced in patients with cancer. (*A*) Summary of the frequency of $CD133^+$ cells in the peripheral blood and frequency of the $CD3^+CD33^+$ subset in gated $CD133^+$ cells. (*B*) Flow cytometric profile of representative subsets gated by CD3 and CD33, or by CD3 and CD14 in $CD133^+$ cells derived from the peripheral blood of healthy adults and patients with cancer. (*C*) Summary of the percentage of different subsets divided by the expression of CD3, CD14, and CD15 markers in $CD133^+$ cells among the peripheral blood of healthy adults ($n = 39$) and patients with cancer ($n = 45$). G, $CD15^+$ cells; L, $CD3^+$ cells; LG, $CD3^+CD15^+$ cells; LM, $CD3^+CD14^+$ cells; M, $CD14^+$ cells; MG, $CD14^+CD15^+$ cells. The white column shows the average frequency of the indicated subsets (lineage alone), and the shaded part shows the frequency of the $CD3^+CD14^+CD15^+$ subset in $CD133^+$ cells. CxCa, cervical cancer; GC, gastrointestinal cancer; HCC, hepatocellular carcinoma; LC, lung cancer; NC, middle-aged healthy donors (*$P < 0.05$ and ***$P < 0.0001$ vs. healthy donors).

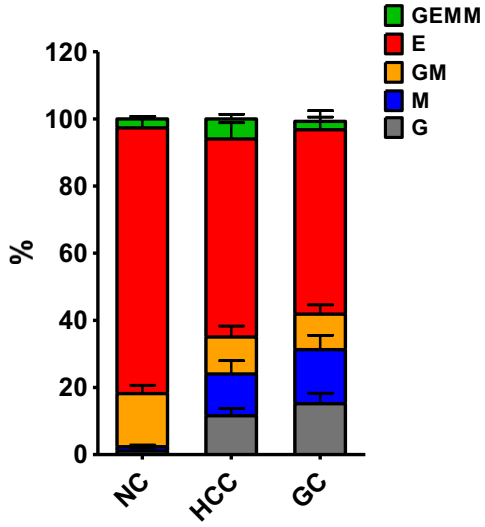

Fig. S3. Increased myeloid differentiation capacity of HSPCs from peripheral blood of patients with cancer. $Lin^{-}CD34^{+}$ cells were isolated from 5 mL peripheral blood of healthy donors and patients with cancer. The isolated cells were plated in methylcellulose-based media. The types and frequency of colonies were counted after 14–16 d of incubation. Summary of the frequency of Lin-CD34+ cells that formed multipotent (GEMM), erythroid (E), granulocyte–monocyte (GM), monocyte (M), or granulocyte (G) colonies in culture from healthy donors (NC, $n = 10$) and hepatocellular carcinoma (HCC, $n = 8$) and colorectal cancer (GC, $n = 12$) patients.

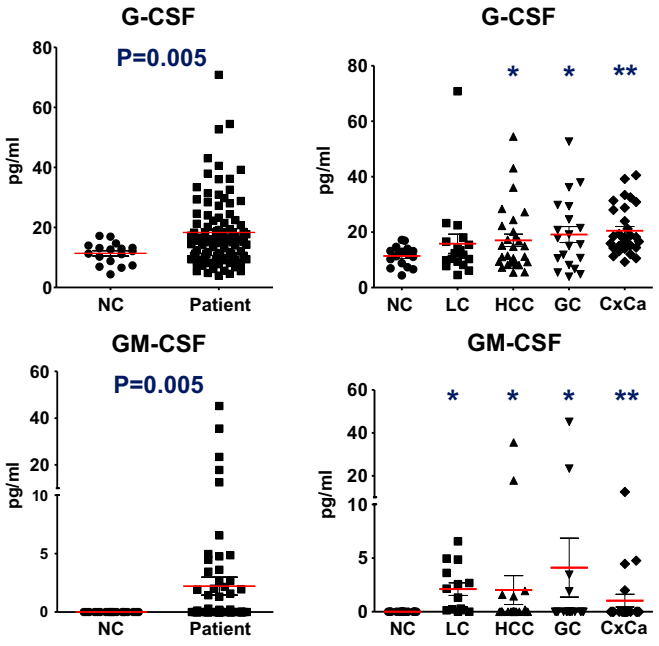

Fig. S4. The concentrations of plasma GM-CSF and G-CSF were elevated in patients with cancer. Plasma levels of GM-CSF and G-CSF in healthy adults and total patients (*Left*) or patients with each type of cancer (*Right*). Each point represents an individual healthy donor ($n = 17$) or patient with cancer ($n = 96$), and horizontal bars represent the group mean values. CxCa, cervical cancer; GC, gastrointestinal cancer; LC, lung cancer; NC, middle-aged healthy donors. Error bars represent SEM (*$P < 0.05$ and **$P < 0.01$ vs. healthy donors).

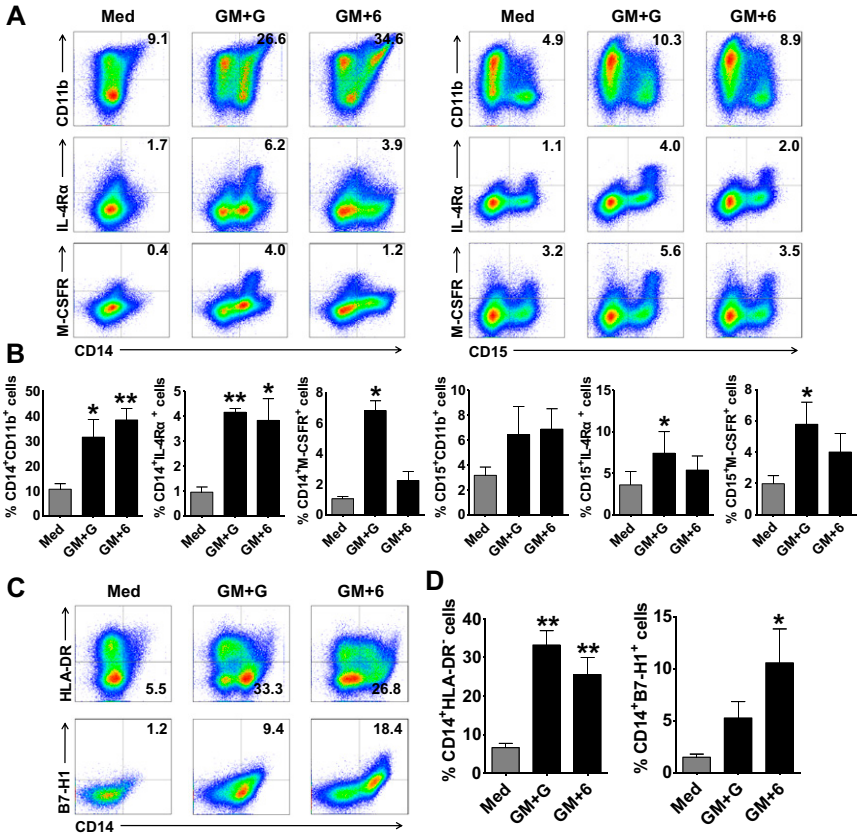

Fig. S5. Human MDSCs can be induced from CB precursors by combined cytokine treatment. The expanded precursors were cocultured at a 1:1 ratio with allogeneic T cells stimulated with 1 μg/mL coated anti-CD3 and 5 μg/mL soluble anti-CD28 for 6 d. (*A*) Representative flow cytometric analysis of CD11b, macrophage colony-stimulating factor receptor (M-CSFR, CD115), and IL-4Rα in expanded cells after stimulation with the combined cytokines. (*B*) Summary of the frequency of $CD11b^+CD14^+$, $CD11b^+CD15^+$, $M\text{-}CSFR^+CD14^+$, $M\text{-}CSFR^+CD15^+$, $IL\text{-}4R\alpha^+CD14^+$, and $IL\text{-}4R\alpha^+CD15^+$ cells in the expanded cells after stimulation with the combined cytokines. (*C*) FACS analysis of HLA-DR and B7-H1 expression on the cells stimulated with the combined cytokines. (*D*) Summary of the frequency of $CD14^+HLA\text{-}DR^-$ and $CD14^+B7\text{-}H1^+$ cells in the expanded cells after stimulation. The data given are the mean (±SE) of four separate experiments (*$P < 0.05$ and **$P < 0.01$ vs. expanded cells cultured in medium alone).

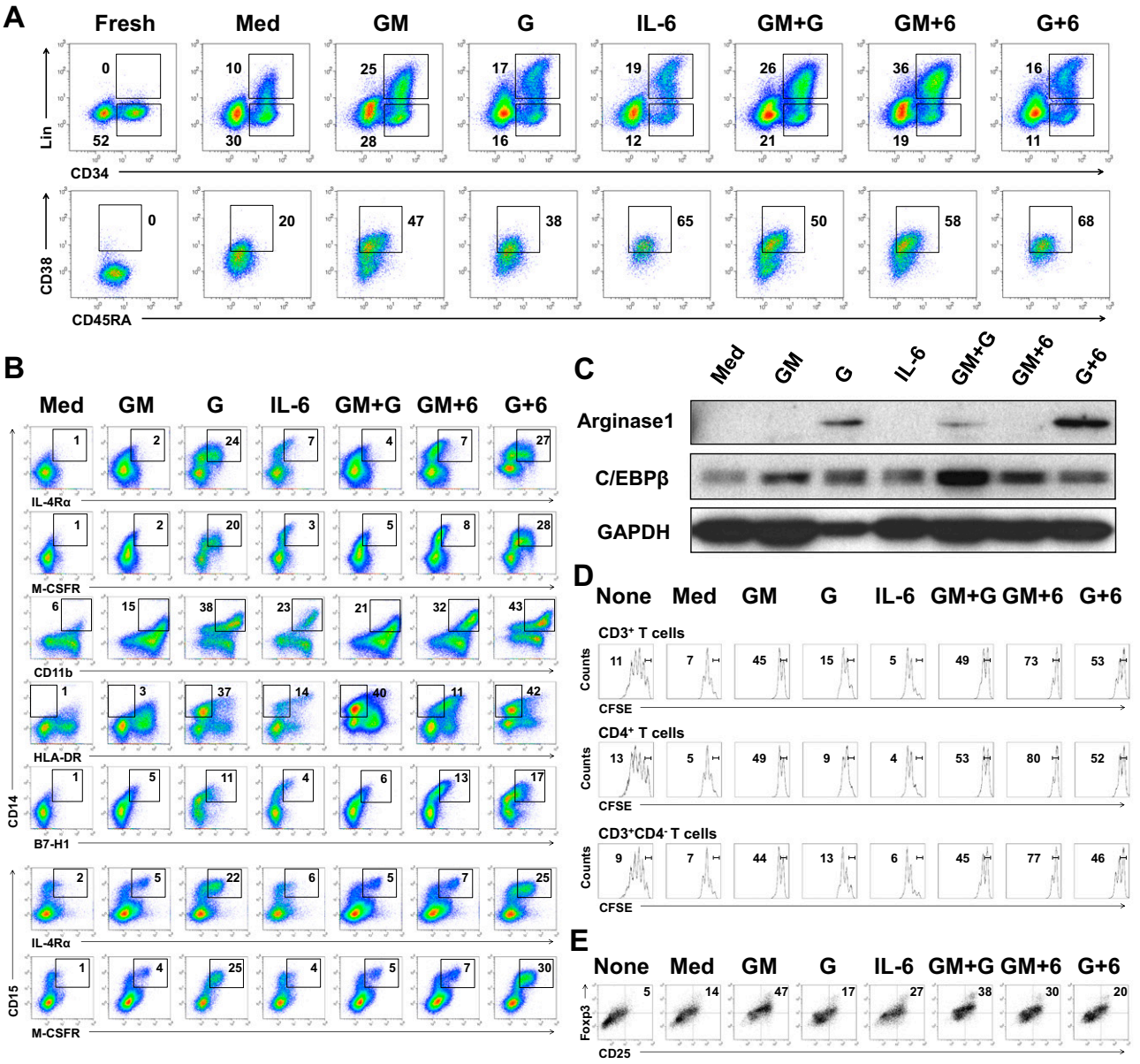

Fig. S6. CB-MDSCs induced by single and combined treatment with cytokines. (*A*) FACS analysis of $Lin^{-}CD34^{+}$ and $Lin^{+}CD34^{+}$ cells and GMPs after stimulation by single and combined cytokines. (*B*) Flow cytometric analysis of CD11b, M-CSFR, IL-4Rα, MHC Class II (HLA-DR), and programmed death ligand 1 (PD-L1, B7-H1) expression on cells stimulated with single and combined cytokines. (*C*) Immunoblot for Arginase1 and CCAAT/enhancer-binding protein beta (C/EBPβ) in stimulated cells by single and combined cytokines. (*D*) FACS analysis of the percentages of the undivided T cells after 6 d of coculture at a 1:1 ratio with or without CB-MDSCs. (*E*) FACs analysis of the percentages of induced $CD25^{+}Foxp3^{+}$ T cells after 6 d of coculture with or without CB-MDSCs. One of two representative experiments is shown.

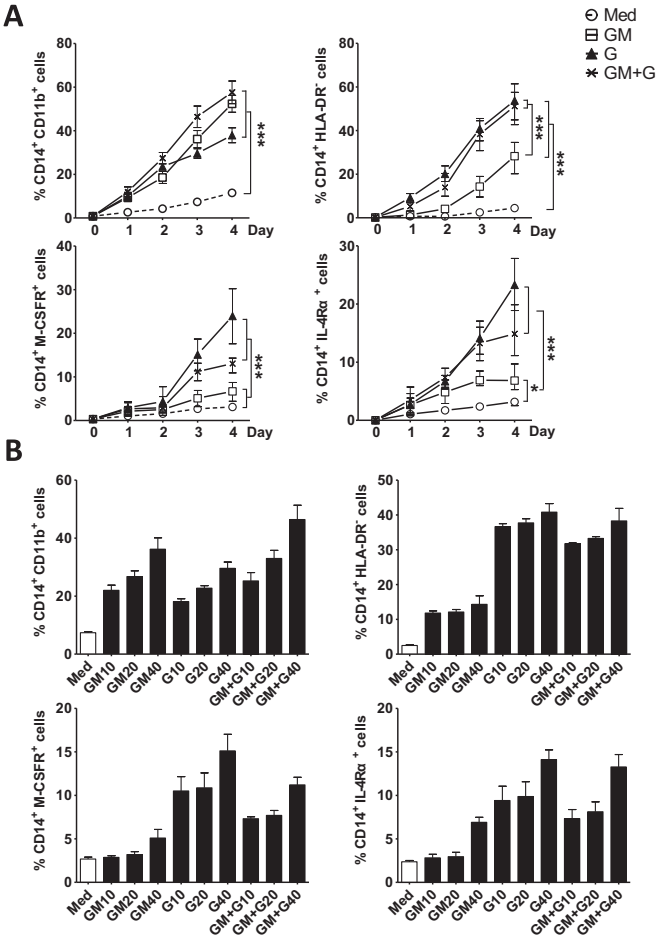

Fig. S7. Kinetic and dose effects of GM-CSF and G-CSF on differentiation of CB-derived progenitors. (*A*) The expanded CB-derived $CD34^+$ cells were treated with GM-CSF (40 ng/mL) and G-CSF (40 ng/mL) alone or in combination for the indicated times and analyzed by FACS. (*B*) The expanded CB-derived $CD34^+$ cells were incubated for 3 d with GM-CSF and G-CSF at the indicated concentrations (in nanograms per milliliter). The data shown represented the mean (±SE) of four separate experiments (*$P < 0.05$, **$P < 0.01$, and ***$P < 0.001$).

Table S1. Characteristics of patients with cancer and healthy donors

Detail (no. of pts.)	Median age, range, y	Sex, male/female
Tumor type		
Breast cancer (9)	50, 27–55	0/9
Colorectal cancer (38)	56, 35–79	27/11
HCC (62)	49, 35–86	52/10
Ovarian cancer (4)	54, 51–61	0/4
Lung cancer (13)	56, 42–68	11/2
Esophagus cancer (4)	51, 48–57	4/0
Cervical cancer (23)	43, 24–71	0/23
Healthy donor		
Young (17)	29, 20–35	11/6
Middle age (79)	51, 36–65	36/43
Elderly (16)	73, 66–91	5/11

Table S2. Technical specifications of antibodies used in our study

Antigen	Specificity	Conjugation	Clone	Source	Cat. No.	App
Lineage mixture 1	Human	FITC	Mix	BD Biosciences	340546	FC
CD133/2	Human	PE	293C3	Miltenyi Biotec	130–090-853	FC
Mouse IgG2b	Mouse	PE	IS6-11E5.11	Miltenyi Biotec	130–092-215	FC
CD117	Human	APC	104D2	eBioscience	17–1178	FC
CD38	Human	PE	HIT2	BD Pharmingen	555460	FC
Mouse IgG1	Mouse	PE	MOPC-21	BD Pharmingen	555749	FC
CD34	Human	PECy7	4H11	eBioscience	25–0349	FC
CD90	Human	APC	5E10	BD Pharmingen	559869	FC
CD127	Human	AF647	HIL-7R-M21	BD Pharmingen	558598	FC
CD123	Human	APC	7G3	BD Pharmingen	560087	FC
CD45RA	Human	EF450	HI100	eBioscience	48–0458	FC
Lineage mixture	Mouse	APC	Mix	BD Pharmingen	558074	FC
CD16/CD32	Mouse	PE	2.4G2	BD Pharmingen	553145	FC
CD135	Mouse	PE	A2F10.1	BD Pharmingen	561068	FC
CD127	Mouse	PECy7	SB/199	BD Pharmingen	560733	FC
CD34	Mouse	FITC	RAM34	BD Pharmingen	560238	FC
Sca-1	Mouse	AF700	D7	eBioscience	56–5981	FC
CD117	Mouse	BV421	2B8	BioLegend	105827	FC
CD3	Human	ECD	UCHT1	Beckman Coulter	A07748	FC
CD14	Human	FITC	RMO52	Beckman Coulter	IM0645U	FC
CD15	Human	EF450	HI98	eBioscience	48–0159	FC
CD4	Human	PECy7	SFCI12T4D11	Beckman Coulter	6607101	FC
CD4	Human	EF450	OKT-4	eBioscience	48–0048	FC
CD33	Human	APC	D3HL60.251	Beckman Coulter	IM2471	FC
CD33	Human	PECy7	D3HL60.251	Beckman Coulter	A54824	FC
CD115	Human	APC	61708	R&D	FAB329A	FC
CD124	Human	APC	25463	R&D	MAB230	FC
CD274	Human	PE	MIH1	BD Pharmingen	557924	FC
CD3Ɛ	Human	APC	APA1/1	BD Pharmingen	558257	FC
CD247	Human	PE	K25-407.69	BD Phosflow	558448	FC
PD-1	Human	APC	J105	eBioscience	12–2799	FC
CD25	Human	PE	BC96	eBioscience	12–0259	FC
Foxp3	Human	APC	236A/E7	eBioscience	17–4777	FC
CD133	Human	Unconjugated	Polyclonal	Abcam	Ab19898	IF
CD15	Human	Unconjugated	MY-1	Thermo scientific	MA1-25926	IF
CD34	Human	Unconjugated	QBEND-10	Abcam	Ab8536	IF
CXCR4	Human	Unconjugated	UMB2	Epitomics	3108–1	IF
Mouse IgG	Mouse	Unconjugated	Polyclonal	Life technologies	A11001	IF
Rabbit IgG	Rabbit	Unconjugated	Polyclonal	Life technologies	A11011	IF